Nova Biotechnol Chim (2022) 21(2): e1267
DOI: 10.36547/nbc.1267

Nova Biotechnologica *et* Chimica

Adsorption of Zn (II) ions from refinery wastewater by sulfuric acid-modified bentonite: Kinetic and isotherm studies

Dihia Bellache[1,2,✉], Karim Moussaceb[2], Jean-Claude Bollinger[3], Farouk Boudrahem[4]

[1]*Department of Process Engineering, Faculty of Science and Applied Science, University of Bouira, 10000 Bouira, Algeria*
[2]*Laboratory of Materials Technology and Process Engineering), Faculty of Technology, A/MIRA Bejaia University, Targa-Ouzemour Road, 06000 Bejaia, Algeria*
[3]*Water Soil Environment Research Group, University of Limoges, 87060 Limoges, France*
[4]*Environmental Engineering Laboratory, Faculty of Technology, A/MIRA Bejaia University, Targa-Ouzemour Road, 06000 Bejaia, Algeria*

✉*Corresponding author:* d.bellache@univ-bouira.dz

Article info

Article history:
Received: 17th November 2021
Accepted: 7th February 2022

Keywords:
Adsorption
Bentonite
Isotherm
Kinetic
Wastewater
Zinc

Abstract

A local bentonite clay from Maghnia (Algeria) was activated with chemical method characterized and tested for its ability to adsorb Zinc (II) from refinery wastewater. Batch experiments were conducted to study the effects of the main parameters such as contact time, initial metal concentration and agitation speed on the adsorption of Zn (II) by local bentonite clay. Experiences have led to the following results: an adsorption rate of the order of 98 % with operating conditions of pH = 4.5, agitation speed of 400 rpm and temperature of 25 ºC. Pseudo-first-order, pseudo-second-order and intraparticle diffusion models were used to analyze the kinetic data obtained at different concentrations. The pseudo-second-order kinetic model agrees very well with the experimental results. In order to determine the best-fit isotherm, in the studied concentration range of Zn(II) at 25 ºC, the experimental equilibrium data were analyzed using tow adsorption isotherm models: Langmuir and Freundlich models, these two models give a good fit.

Introduction

A number of industries, such as metal plating facilities, mining operations, tanneries, nuclear power plants, fertilizers and battery productions, often discharges heavy metals, this can lead to the contamination of freshwater and marine environment (Low and Lee 2000). Metal ions in water can occur naturally from anthropogenic sources and from leaching of ore deposits, which mainly include solid waste disposal and industrial effluents. The levels of heavy metals in water system have substantially increased over time with rapid development of industrial activities (Nouri *et al.* 2006).

The main sources of zinc in the environment are the manufacturing of brass and bronze alloys and galvanization (Arias and Sen 2009). It is also utilized in paints, rubber, plastics, cosmetics, and pharmaceuticals. Zinc is an essential element for life and act as micronutrient when present in trace amounts, the maximum daily dose not to be exceeded is 40 mg for an adult. However, high zinc can cause eminent health problems, such as stomach cramps, vomiting, skin irritations, anemia, and nausea (Zwain 2012).

Various methods are available to remove and isolate these heavy metals from water and wastewater such as ion exchange, chemical precipitation, membrane filtration, adsorption, and electrochemical treatment technologies (Fu and Wang 2011). Adsorption is very promising because of the advantages of easy operation, low cost, and possibility of metal recovery (Dang *et al.* 2021). These methods have proven their ability in removing heavy metals from wastewater; however, several factors need to be considered when choosing the appropriate method. Adsorption has been proven to have better performance compared to other methods as mentioned in many studies (Kamari *et al.* 2014)

The adsorption ability of clay is caused by a net negative charge on the structure of fine grain silicate minerals. This negative charge is neutralized by the adsorption of positively charged species, giving clay the ability to attract and hold cations such as heavy metals. The large surface area of clays (up to 800 $m^2.g^{-1}$) also contributes to the high adsorption capacity, there are three basic classes of clays: kaolinite, micas (such as illite), and smectites (e.g., montmorillonite). Of the three species, montmorillonite clays have the smallest crystals, the largest surface area, and the highest cation exchange capacity. Thus, montmorillonite clays would be expected to have the highest adsorption capacity (Haider *et al.* 2014).

Studies such as those conducted by (Bellir *et al.* 2013; Sen *et al.* 2013; Vasconcelos *et al.* 2013) have investigated the potential of bentonite for the removal of zinc ion. Although the results involving zinc removal by bentonite are significant and promising, the properties of adsorbents for optimizing the conditions of the process need to be better understood.

This study explored the feasibility of utilizing an Algerian activated bentonite for the adsorption of zinc from refinery wastewater. Various parameters affecting adsorption process, such as contact time, initial zinc concentration, adsorbent dosages, agitation speed and the medium temperature were investigated. The kinetic adsorption results have been analyzed using both pseudo-first-order and pseudo-second-order kinetics models. The mechanism of adsorption process has been explained based on intra-particle diffusion model. Finally, the Langmuir and Freundlich models were applied for the analysis of the adsorption equilibrium.

Experimental

Characteristics of refinery wastewater

The main physicochemical parameters on the quality of refinery wastewater are shown in Table 1. The determination of these parameters is performed according to standard analytical methods (Rodier *et al.* 2009). Based on this table, the physicochemical characteristics of the refinery water are within the limits of wastewater standards, except COD and chloride and zinc concentrations that exceed current standards.

Table 1. Physical-chemical characteristics of refinery wastewater and the OMS limit values of wastewater parameters.

Parametres	**Values**	**Normes**
pH	7.07	6,5 – 8,5
Conductivitym S/Cm	40.89	2,8
Turbidity (NTU)	85.6	5 – 30
TSS [$mg.L^{-1}$]	387.8	30
COD [$mg.O_2.L^{-1}$]	1601.24	120
Chloride [$mg.L^{-1}$]	2098.03	200
Sulfate [$mg.L^{-1}$]	33.18	250
Chromium (VI) [$mg.L^{-1}$]	0.02	0,1
Lead [$mg.L^{-1}$]	0.04	0,5
Zinc [$mg.L^{-1}$]	6.7	3

COD – Chemical Oxygen; TSS – Total Suspended Solids.

Characteristic of raw bentonite

In this study, bentonite obtained from Maghnia (North-Western part of Algeria) and supplied by ENOF “National Company of useful and non-ferrous products, Algeria” was used as an adsorbent. Its chemical and physico-chemical characteristics are summarized in Table 2 and Table 3.

Preparation of acid-activated bentonite

The Na-bentonite was prepared with a procedure similar to already reported (Khalaf *et al.* 1997). 30 g of crude bentonite was mixed with 1 L of 1 M NaCl solution and stirred for 24 h. After three successive treatments, the homoionic bentonite was dialyzed in deionized water until it was free of chloride. Then it was separated by centrifugation to eliminate all other solid phases (quartz, and calcite) Boutahala and Tedjar 1993).

In a conical flask, 50 g of purified bentonite and 250 mL of sulfuric acid solution (0.5 M and 1 M). The mixture was homogenized and allowed to stand at room temperature for 24 h. The resulting activated clay was centrifuged and washed with distilled water several times until it was free of SO_4^{2-} as indicated by the $AgNO_3$ test and was then dried at 100 – 107 °C for 24 h. Acid-activated bentonite with different concentration of sulfuric acid at 0.5 M end 1 M are noted respectively B05 and B1, was then stored for further use in the adsorption tests.

Table 2. Chemical composition of bentonite sample.

Constituent	SiO_2	MgO	Al_2O_3	K_2O	CaO	F_2O_3	Na_2O	TiO_2	As
Weight [%]	69.4	1.1	14.7	0.8	0.3	1.2	0.5	0.2	0.05
Loss of ignitions = 11									

Table 3. Physico-chemical properties of Bentonite.

Surface area [m².g^{-1}]	CEC [eqg^{-1}]	pH	Exchangeable cation [meq/100g]			
			Ca^{2+}	Mg^{2+}	Na^{+}	K^{+}
80	0.97	6.2	30.6	12.8	36.2	9.5

Batch adsorption study

The ability of bentonite to adsorb Zn(II) ions from refinery wastewater was studied under various optimized conditions of concentration of metals, and contact time, adsorbent dosage and strength speed.

Batch adsorption experiments were carried in 250 cm^3 Erlenmeyer flasks with known amount of the adsorbent and 100 mL of solution, with pH = 4.5, the initial pH of the solutions was adjusted with 0.1 M HNO_3 or 0.1 M NaOH to the desired value. The Erlenmeyer were kept at the desired temperature under constant agitation. After 70 min, the suspensions were centrifuged and the solutions were analyzed for Zn(II) ions by atomic absorption spectrometry AA-6501F.

The amount of adsorbed at any time, q_t (mg.g^{-1}), was calculated using Eq. 1:

$$q_t = \frac{C_i - C_t}{m} V \qquad (1)$$

where, C_i and C_t are the initial and liquid-phase concentrations at any time t of Zinc solution (mg.L^{-1}), respectively, V is the volume of wastewater (L) and m is the mass (g) of the adsorbent used.

The removal efficiency, E (%) of the system, is Eq. 2 (Boudrahem *et al.* 2011):

$$E(\%) = \frac{C_i - C_t}{C_i} 100 \qquad (2)$$

Results and Discussion

Adsorbent characterization

The FTIR spectra of natural bentonite and acid activated bentonite were taken in the range of 4,000 – 400 cm^{-1} (Shimadzu FTIR-8400, SHIMADZU Corp., Tokyo, Japan). FTIR spectra are illustrated in Fig. 1 and 2. Positions and assignment of the vibrational bands of this clay are shown in Table 4. The broad and slight bands at 3,627 and 3,435 cm^{-1} are due to the O–H stretching vibration of the silanol (Si–OH) groups from the solid and H–O–H vibration of the water molecules adsorbed on the silicate surface. The band at 1,634.5 cm^{-1} reflects the bending H–O–H bond of water molecules, which is retained in the silicate matrix. The most intensive and sharp band at 1,039 cm^{-1} represents the Si–O–Si groups of the tetrahedral sheets. Where the bands around 515 and 523 cm^{-1} is are ascribed to Si–O–Al (where Al is the octahedral cation) and to Si–O–Si bending vibration. Furthermore, the sharp bands at 790 with reflexion at 778.4 cm^{-1} confirm the presence of quartz admixtures in the sample (Tomic *et al.* 2011).

FTIR spectroscopy is very sensitive to modification of the clay structure upon acid treatment, as illustrated in Fig. 1. In FTIR-spectrum of the acid activated bentonite, weakening of absorption band intensity at 3,437 and 1,639 cm^{-1} is marked (Fig. 2). It corresponds to the process of removal of interlayer water (Schrader and Loeb 1992). Absorption peaks between 3,435 and 3,627 cm^{-1} are due to stretching bands of the OH groups.

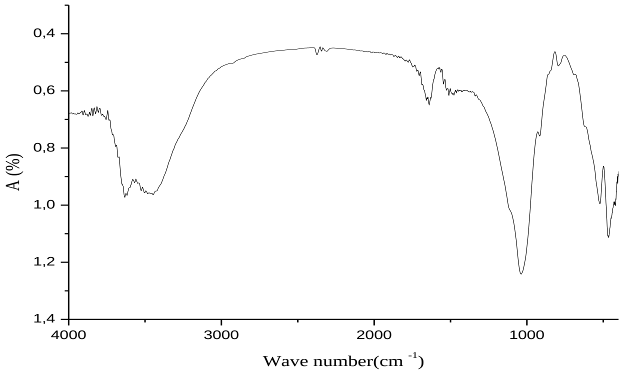

Fig. 1. FTIR spectrum of raw bentonite.

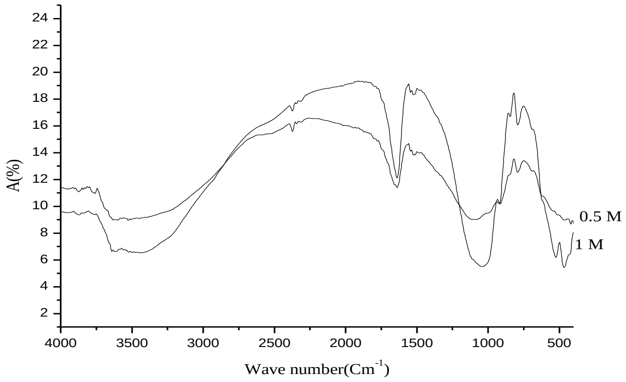

Fig. 2. FTIR spectrum of acid activated bentonites.

While the band at 1,639 cm^{-1} corresponds to the OH deformation of water to observe natural bentonite and acid activated bentonite, but the peak intensities of both the acid-activated bentonites are lower than that of natural bentonite.

Absorption band reduction at 3,627 cm^{-1} indicates development of dehydroxylation process. This is believed to occur as a result of acid activation of bentonite (Ozcan and Ozcan 2004).

In addition, the transformation of the tetrahedral sheet was found at 781 cm^{-1} and 783 cm^{-1} for B1 and B05 activated bentonites respectively. The acid activation leads to the formation of amorphous silica, indicated by the increased intensity of the peak, which may expose more adsorption sites (Komandel *et al.* 1990).

Table 4. FTIR band assignments of raw and activated bentonites.

Maxima [cm^{-1}]	**Assignements**
3,627 et 3,435	–OH stretching
3,443	–OH stretching, hydratation
1,637 et 1,639	–OH stretching, hydratation
1,039 et 1,038	Si–O stretching (in plane)
523 et 515	Si–O–Al bending
477 et 458	Si-O-Si
790 et 799	Quatrz

Effect of contact time and initial Zn (II) concentration on the adsorption

Fig. 3 represents a plot of the amount of zinc metal ion adsorbed ($mg.g^{-1}$) versus contact time for Zn-B05 and Zn-B1 system at different initial metal ion concentration range.

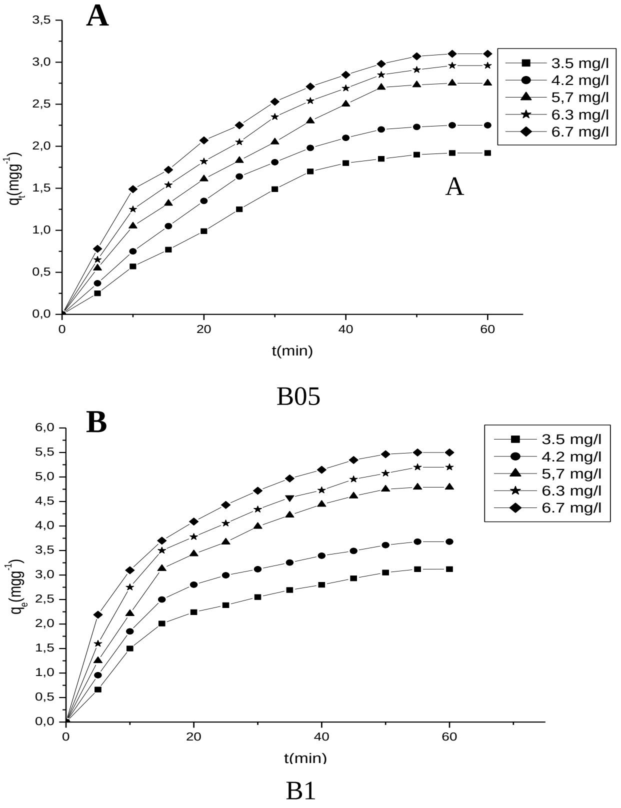

Fig. 3. Effect of contact time on Zn (II) metal ion adsorption by B05 (**A**) and B1 (**B**) for different initial Zn (II) ions concentration. Conditions: pH = 4.5; adsorbent dose = 1 $g.L^{-1}$; agitation speed = 400 rpm and T = 25 ºC.

From these plots, it is found that the amount of adsorption i.e. mg of adsorbate per gram of adsorbent increases with increasing of contact time at all initial metal ion concentrations and equilibrium is attained within 50 min for both the systems further it was observed that the amount of metal ion uptake, q_t ($mg.g^{-1}$) is increased with increase in initial metal ion concentration. The increase in adsorption is more pronounced for Zn-B1 system compared to Zn-B05 system the difference in the zinc sorption onto the bentonites may be due to the difference in the mineralogical compositions and associated cations in the exchangeable sites (Sheta *et al.* 2003).

These kinetic experiments clearly indicate that the adsorption of Zn (II) on acid activated clay surface is a two-step process: a rapid adsorption of metal ions to the external surface is followed by possible slow intraparticle diffusion in the interior of the particles (Sen and Sarzali 2008). This two-stage process is also due to the presence of two different types of binding sites on the adsorbents. The two-stage sorption mechanism with the first rapid and quantitatively predominant and the second slower and quantitatively insignificant, has been extensively reported in literature (Yang *et al.* 2010).

Effect of agitation speed

The experiments were undertaken with different agitation speeds of (200, 400, 600,800 and 1,000) rpm keeping constant the other process variables. Fig. 4 show that the high amount of Zn(II) ions adsorbed at equilibrium (5.5 and 3.1 $mg.g^{-1}$ for B1 and B05, respectively) is obtained with an agitation speed of 400 rpm for both adsorbents. The adsorbed amount of Zn(II) increases with an increase of the agitation speed from (200 to 400) rpm, and at higher stirring speed (> 400 rpm), the sorbed amount of Zn(II) decreases. When increasing the agitation speed (< 400 rpm), the diffusion rate of metal ions from the bulk liquid to the liquid boundary layer surrounding sorbent particles becomes higher because of an enhancement of turbulence and a decrease of the thickness of the liquid boundary layer. At higher stirring speeds (> 400 rpm), the decrease of the sorbed amount of Zn(II) is attributed to the rejection of the adsorbent part, which is found plated against the internal walls of the reactor (Boudrahem *et al.* 2011).

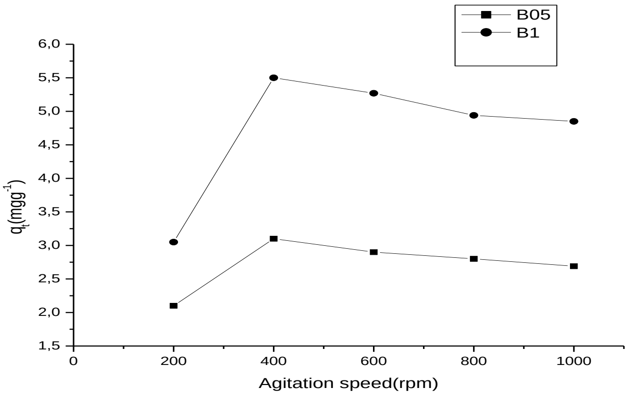

Fig. 4. Effect of agitation speed on the sorption of Zinc by both activated clay B1 and B05. Conditions: pH = 4.5; initial concentration of Zn(II) = 6.7 $mg.L^{-1}$ and T = 25 °C.

Effect of adsorbent dosage

The effect of adsorbent dosage on the adsorption of zinc (II) was studied at different dosages in the solution at pH 4.5. As shown in Fig. 5, the adsorption percentage of zinc (II) removed ions increased as the dosage of bentonite increased from 1.0 to 3.0 $g.L^{-1}$. This may be explained by the metal ions competing for limiting adsorption sites at a lower bentonite dosage.

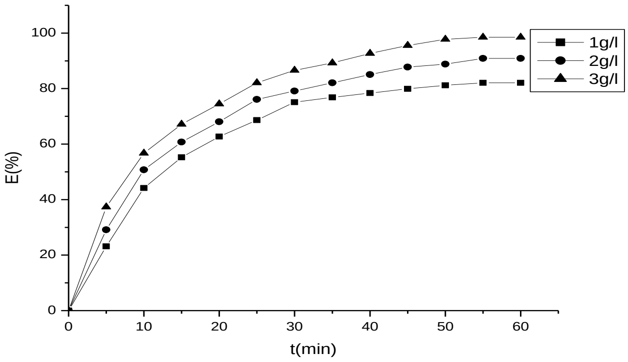

Fig. 5. Effect of dosage of B1 activated bentonite on the sorption of Zinc. Conditions: pH = 4.5; initial concentration of Zn(II) = 6.7 $mg.L^{-1}$ and temperature = 25 °C.

The increase in the adsorption percentage with an increase in adsorbent dosage was due to an increase in active sites on the adsorbent, thus facilitating the penetration of metal ions to the sorption sites (Sarı *et al.* 2007a; 2007b). These observations agree with others reported in the literature for the adsorption of metals ions by different materials (Mishra and Patel 2009).

Effect of the medium temperature

Fig. 6 shows that the effect of temperature on the retention of Zn(II) ions is explained by the fact that an increase in temperature leads to a moderately considerable increase in the adsorption capacity, and which becomes increasingly less effective after 15 min of contact, the elimination rate curves for different temperatures become superimposed. The increase in temperature provides energy for the ionic particles which in turn allows them to surpass the repulsion forces with the supports up to a certain limit, beyond which the temperature becomes ineffective “state of saturation”. It can be seen from the analysis of Fig. 6 that the bentonite removal rate reaches approximately 82 % for all temperatures studied.

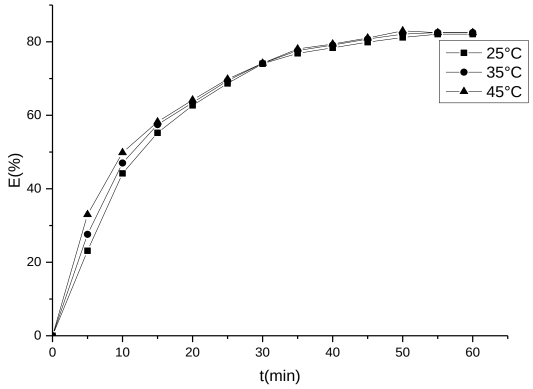

Fig. 6. Effect of dosage of B1 activated bentonite on the sorption of Zinc. Conditions: pH = 4.5; initial concentration of Zn(II) = 6.7 mg.L^{-1}, adsorbent dose = 1 g.L^{-1}, agitation speed = 400 rpm.

Adsorption kinetics

The kinetics of adsorption describes the rate of metal ions uptake on activated Bentonites and this rate controls the equilibrium time. The kinetics of adsorbate uptake is required for selecting optimum operating conditions for the full-scale batch process (Gupta *et al.* 1997).

The kinetic parameter, which is helpful for the prediction of adsorption rate, gives important information for designing and modelling the processes. The kinetics of the adsorption data was analyzed using different kinetic models, such as pseudo-first-order and pseudo-second-order models.

Pseudo-first-order model

The kinetic data were treated with the Lagergren first-order model Eq. 3 (Lagergren 1898):

$$\frac{dq_t}{dt} = k_1(q_e - q_t) \qquad (3)$$

where k_1 is the adsorption rate constant for the first order adsorption, $q_t$is the amount of heavy metal adsorbed at time t (mg.g^{-1}) and q_e is the amount of heavy metal adsorbed at saturation (mg.g^{-1}).
The integration of the Eq. 3 gives the following expression Eq. 4:

$$\ln[(q_e - q_t)] = -k_1 t + C_1 \qquad (4)$$

where C_1 is the integration constant for first order reaction kinetic.
If it is supposed that q = 0 at t = 0, then (Eq. 5):

$$\ln[(q_e - q_t)] = \ln q_e - k_1 t \qquad (5)$$

Values of adsorption rate constant k_1 for the zinc(II) adsorption onto acid activated bentonites (B1, B05) were determined from the straight-line plot of $\ln[(q_e - q_t)]$ against t. The data were fitted with a poor correlation coefficient (Table 5), indicating that the rate of removal of zinc onto both acid-activated bentonites does not follow the pseudo first-order equation.

Pseudo-second-order reaction kinetic

Adsorption data was also evaluated according to the Pseudo second-order reaction kinetic proposed by Ho and McKay (Ho and McKay 1998; Eq. 6):

$$\frac{dq_t}{dt} = k_2(q_e - q_t)^2 \qquad (6)$$

where k_2 is the second order reaction constant. If Eq. 6 is integrated, the following expression is obtained (Eq. 7):

$$\frac{1}{(q_e - q_t)} = k_2 t + C_2 \dots \qquad (7)$$

In Eq. 7, C_2 is the integration constant of the second order reaction kinetic. With an algorithmic arrangement, the following statement is formed (Eq. 8):

$$\frac{t}{q_t} = \frac{1}{K_2 {q_e}^2} + \frac{1}{q_e} t \qquad (8)$$

The pseudo second order model can be determined experimentally by plotting t/qt against t, and the constants q_e and K_2 obtained from the slope and intercept.

The pseudo second order kinetic parameters and the R^2 value obtained are given in Table 5. This model can thus be applied to the adsorption data, as indicated by the good R^2 value obtained. This implies that the rate-limiting step is a chemisorption involving valency forces caused by sharing or exchange of electrons between sorbent and sorbate species in solution (Unlu and Ersoz 2006). The pseudo second order model have been reported to give very good fits to experimental data by many researchers (Sarı *et al.* 2007a; 2007b).

Table 5. Calculated kinetic parameters for pseudo first-order and second order for the adsorption of zinc onto acid activated bentonites.

	Adsorbent	**Concentration [mg.L^{-1}]**	**$q_{e exp}$ [mg.g^{-1}]**	**k [g.mg^{-1}.min^{-1}]**	**$q_{e cal}$ [mg.g^{-1}]**	**R^2**
Pseudo-first-orderkinetic	**B05**	3.500	1.920	0.085	3.414	0.911
		4.200	2.250	0.088	3.857	0.916
		6.700	3.100	0.079	4.275	0.909
	B1	3.500	3.120	0.066	3.421	0.955
		4.200	3.680	0.07	3.849	0.968
		6.700	5.500	0.084	6.61	0.915
Pseudo-second-orderkinetic	**B05**	3.500	1.920	0.001	5.649	0.781
		4.200	2.250	0.004	4.587	0.939
		6.700	3.100	0.010	4.424	0.994
	B1	3.500	3.120	0.0107	4.366	0.975
		4.200	3.680	0.0123	4.807	0.990
		6.700	5.500	0.012	6.666	0.998

Adsorption mechanism

Generally, any sorption process can be described by the following three steps: (i) film or surface diffusion, (ii) intraparticle or pore diffusion and (iii) sorption on the interior sites of the sorbent. Since the last step is very rapid, it is assumed that it does not influence the overall kinetics. The rate of adsorption process, therefore, will be controlled by either film diffusion or intraparticle diffusion depending on which step is slower. The Weber–Morris intraparticle diffusion model has often been used to determine if intraparticle diffusion is the rate-limiting step. The intraparticle diffusion equation can be written by following Eq. 9:

$$q_t = k_d t^{1/2} \qquad (9)$$

where k_d is the intraparticle diffusion constant (mg.g^{-1}.min$^{-1/2}$). According to this model, the plot of q_t versus the square root of time t $^{1/2}$ should be linear if intraparticle diffusion is involved in the adsorption process and if the plot passes through the origin, then intraparticle diffusion is the sole rate-limiting step. It has also been suggested that in instances when the plot is multilinear two or more steps govern the adsorption process (Boparai and Joseph 2011).

Linear plots of the intraparticle diffusion model are shown in Fig. 7 and Table 6. For both B05 and B1 acid activated bentonite, the adsorption process can be divided into three stages; the initial first-shape portion of the curve corresponds to the external surface adsorption stage or instantaneous adsorption stage. The second, gradual linear portion corresponds to intraparticle diffusion, and the final represents the equilibrium stage.

Therefore, Zn(II) adsorption on both acid activated bentonites can be considered as the combination of surface adsorption and pore-filling by diffusing.

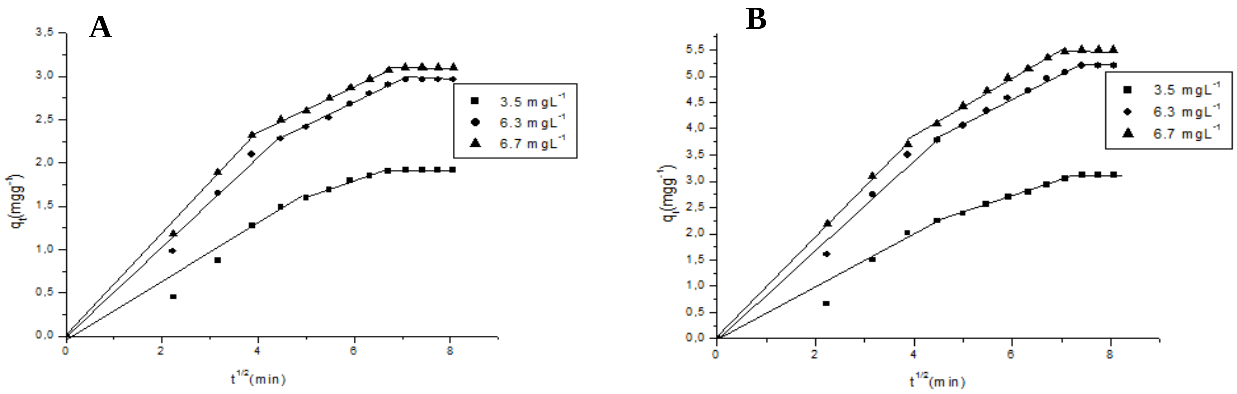

B05 B1

Fig. 7. Intraparticle diffusion plot for Zn (II) adsorption onto acid activated bentonites; Condition: pH = 4.5; agitation speed = 400 rpm and T = 25 ºC.

Table 6. Calculated parameters of intraparticle diffusion for the adsorption of zinc onto acid activated bentonites.

Adsorbents	**Concentration [mg.L^{-1}]**	**K$_{d1}$ [g.mg^{-1z}.min$^{-1/2}$]**	**R$_1^2$**	**K$_{d2}$ [g.mg^{-1}.min$^{-1/2}$]**	**R$_2^2$**
B05	3.500	0.311	0.954	0.159	0.963
	4.200	0.362	0.987	0.200	0.975
	6.700	0.586	0.993	0.252	0.993
B1	3.500	0.480	0.943	0.306	0.998
	4.200	0.604	0.963	0.299	0.997
	6.700	0.967	0.999	0.523	0.981

Adsorption Langmuir isotherm

The theoretical Langmuir sorption isotherm is based on the assumption that the maximum adsorption occurs when a saturated monolayer of solute molecules is present on the adsorbent surface, the energy of adsorption is constant and there is no migration of adsorbate molecules in the surface plane. The Langmuir isotherm model is expressed as follows Eq. 10 (Langmuir 1918):

$$q_e = q_m \times \left[\frac{k_L C_e}{1 + k_L C_e}\right] \qquad (10)$$

where k_L is the Langmuir constant (L.mg^{-1}) and q_{max} is the maximum adsorption capacity (mg.g^{-1}).

The linearized Langmuir equation is (Eq. 11):

$$\frac{C_e}{q_e} = \frac{1}{q_m} C_e + \frac{1}{k_L q_m} \qquad (11)$$

The Langmuir constants, q_m (maximum adsorption capacity) and k_L, can be obtained from plots between C_e/q_e versus C_e, with fixed initial conditions. Overall, Langmuir isotherm model has a high regression coefficient (R^2) for both the systems. The amount of metal adsorbed at equilibrium, adjusted by Langmuir model, was 8.4 mg.g^{-1} for the B1 activated clay and 5.64 mg.g^{-1} for the B05 activated clay.

Table 7. Langmuir parameters obtained from Langmuir plots.

Adsorbent	**T [ºC]**	***q_{max}* [mg.g^{-1}]**	***k_L* [mg^{-1}]**	***R^2***	***R_L* [mg.L^{-1}]**		
					3.5	4.2	6.7
B05	25°C	5.64	0.33	0.994	0.46	0.41	0.31
B1	25°C	8.40	1.52	0.996	0.15	0.13	0.08

The essential characteristics of the Langmuir isotherm can be expressed in terms of dimensionless constant separation factor or equilibrium parameter, R_L which is defined by Eq. 12 (Hall *et al.* 1966):

$$R_L = \frac{1}{1 + C_i K_L} \qquad (12)$$

The dimensionless separation factor (R_L) was calculated, based on Langmuir constant k_L and the initial zinc concentration presented in Table 7 for both the systems. These R_L values indicates favorable adsorption as it lie in the range $< 0 < R_L < 1$ (Sen and Dustin 2011).

Adsorption Freundlich isotherm

In 1906, Freundlich presented the earliest known sorption isotherm equation (Veli and Alyuz 2007). This empirical model can be applied to non-ideal sorption on heterogeneous surfaces as well as multilayer sorption and is expressed by the following equation (Eq. 13):

$$q_e = k_F \times C_e^{\frac{1}{n}} \qquad (13)$$

where C_e (mg.L^{-1}) is the equilibrium concentration and q_e (mg.g^{-1}) is the amount adsorbed of zinc per unit mass of the adsorbent. The constant n is the Freundlich equation exponent that represents the parameter characterizing quasi-Gaussian energetic heterogeneity of the adsorption surface (Bansal and Goyal 2005). KF (mg$^{1-(1/n)}$.L$^{1/n}$ .g^{-1}) is the Freundlich constant indicative of the relative adsorption capacity of the adsorbent.

The Freundlich exponent, n, should have values lying in the range of 1 – 10 for classification as favorable adsorption (H.M.F. 1906). The linear form of this model is given by Eq. 14:

$$Ln\,q_e = \frac{1}{n} Ln\,c_e + Ln\,k_F \qquad (14)$$

where k_F and n can be calculated from the intercept and slope between ln (q_e) and ln (C_e) which are shown in Table 8 for both the systems. The value of R^2 obtained confirms the applicability of the Freundlich isotherm to the sorption process. The n values are greater than one, which may ndicate that the adsorption of metal ions by the activated bentonite is favorable (EL-Geundi 1990).

Table 8. Freundlich parameters obtained from Freundlich plots.

Adsorbant	T [°C]	n	k_F	R^2
B05	25	1.79	0.414	0.994
B1	25	2.07	1.61	0.999

The comparison of the experimental values with the values of q_e obtained by both models is shown in Fig. 8. As it is seen from this figure, Langmuir isotherms usually fitted better with the experimental data rather than Freundlich isotherms. In addition, some other studies showed that Langmuir and Freundlich isotherms correspond well with the experimental results of some heavy metals (Bereket *et al.* 1997).

Several researchers have studied the adsorption capacity of different sorbents. The comparison of the activated bentonite with various adsorbents, in terms of adsorption capacity for zinc (II) ions from aqueous solution at laboratory, is given in Table 9.

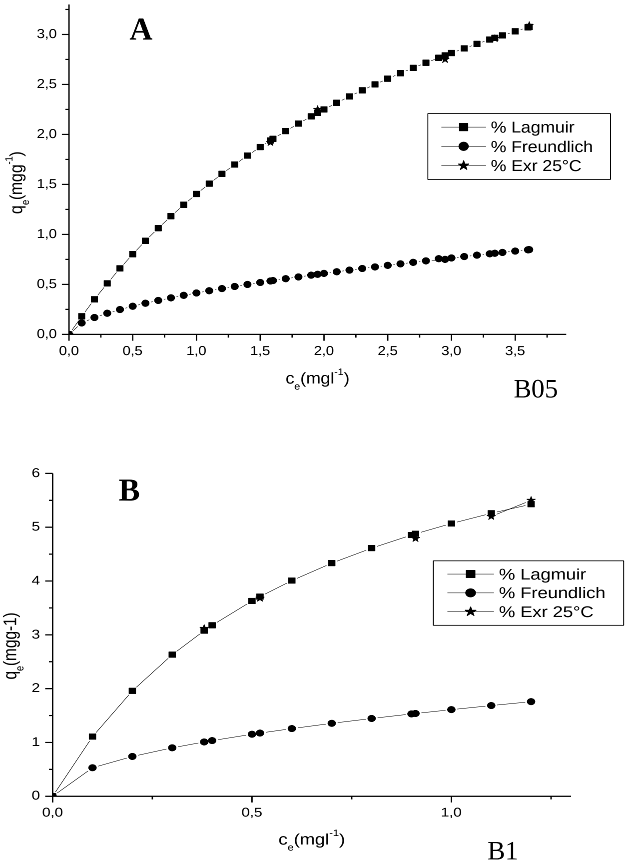

Fig. 8. Sorption isotherms for Zinc onto activated bentonites. Conditions: pH = 4.5; agitation speed = 400 rpm; agitation time = 60 min and temperature = 25 °C.

Several researchers have studied the adsorption capacity of different sorbents. The comparison of the activated bentonite with various adsorbents, in terms of adsorption capacity for zinc (II) ions from aqueous solution at laboratory, is given in Table 9.

Table 9. Values of maximum sorption capacities of some sorbent for Zinc (II).

Sorbent	**Modifying agent [s]**	**Zn(II) [mg.L^{-1}]**	**q_m [mg.g^{-1}]**	**Source**
Bentonite	—	300	52.91	(Tunali and Akar 2006)
Botrytis cinerea	NaOH	100	12.98	(Agrawal *et al.* 2004)
Sea nodule residue	Hydrochloric acid	200	32.46	(Kargi and Cikla 2006)

Conclusion

The present study has evaluated the zinc (II) ions removal potential of an Algerian chemically treated bentonite; the obtained results can be summarized as follows:

In batch adsorption studies, the amount of metal ion Zn (II) adsorption on both clay minerals was found to increase with increase in initial metal ion concentration, contact time and in the mass of clay. The amount of Zn(II) ions adsorbed by both materials increases with increasing initial zinc concentration and contact time. The adsorption capacity of activated bentonite at 1M H_2SO_4 (B1) is higher than that of activated bentonite at 0.5M H_2SO_4 (B05) Stirring rate does not affect the amount of Zn(II) ions adsorbed from 400 rpm for both adsorbents; Zinc removal rate increases with increasing adsorbent mass. The study of the influence of temperature on adsorption showed that the temperature has no influence on the zinc removal rate. High adsorption capacity of acid activates bentonite (B1) compared to acid activate bentonite (B05). Kinetic experiments clearly indicated that sorption of Zn (II) on both activated bentonite is a two steps process: a rapid adsorption of metal ion to the external surface followed by intraparticle diffusion into the interior of adsorbent, which has also confirmed by intraparticle diffusion model. Overall, the kinetic studies revealed that adsorption process followed the pseudo-second-order kinetics model. The Langmuir and Freundlich isotherms models were applicable.

References

Agrawal A, Sahu KK, Pandey BD (2004) Removal of zinc from aqueous solutions using sea nodule residue. Colloids Surf. A 3: 133-140.

Arias F, Sen TK (2009) Removal of zinc metal ion (Zn^{2+}) from its aqueous solution by kaolin clay mineral: A kinetic and equilibrium study, Colloids Surf. A. 348: 100-108.

Bansal RC, Goyal M (2005) Activated carbon adsorption. CRC Press, Boca Raton, USA, 520 p.

Bellir K, Lehocine MB, Meniai AH (2013) Zinc removal from aqueous solutions by adsorption onto bentonite, Desalin. Water Treat. 51: 5035-5048.

Bereket G, Aroguz AZ, Özel MZ (1997) Removal of Pb(II), Cd(II), Cu(II), and Zn(II) from aqueous solutions by adsorption on bentonite. J. Colloid Interface Sci. 187: 338-343.

Boparai HK, Joseph M (2011) Kinetics and thermodynamics of cadmium ion removal by adsorption onto nanozerovalent iron particles. J. Hazard. Mater. 186: 458-465.

Boudrahem F, Aissani-Benissad F, Soualah A (2011) Adsorption of lead(II) from aqueous solution by using leaves of date trees as an adsorbent. Chem. Eng. J. 56: 1804-1812.

Boutahala M, Tedjar F (1993) Application of exchanged montmorillonite as protonic solid electrolyte. Solid State. Ion. 61: 257-263.

Dang J, Wang H., Wang C (2021) Adsorption of toxic zinc by functionalized lignocellulose derived from waste biomass: Kinetics, isotherms and thermodynamics. Sustainability 13: 10673.

EL-Geundi MS (1990) Adsorption equilibria of basic dyestuffs onto maize cob. Adsorp. Sci. Technol. 7: 114.

Fu F, Wang Q (2011) Removal of heavy metal ions from wastewaters: a review. J. Environ. Manag. 3: 407-418.

Gupta VK, Srivastava SK, Mohan D (1997) Removal of lead and chromium by activated slag-A blast-furnace waste. Ind. Eng. Chem. Res. 123: 461-468.

H.M.F. (1906) Activated carbon adsorption. J. Phys. Chem. A. 57: 385-470.

Haider M, Mohammadtaghi Vakili Z, Dahlan I (2014) Waste material adsorbents for zinc removal from wastewater: A comprehensive review. Int. J. Chem. Eng. 1: 1-13.

Hall KR, Eagleton LC, Acrivos A, Vermeulen T (1966) Pore and solid-diffusion kinetics in fixed-bed adsorption under constant-pattern conditions. Ind. Eng. Chem. Fund. 5:

212-223.

Ho YS, McKay G (1998) Sorption of dye from aqueous solution by peat. Chem. Eng. J. 70: 115-124.

Kamari A, Yusoff SNM, Abdullah F, Putra WP (2014) Biosorptive removal of Cu(II), Ni(II) and Pb(II) ions from aqueous solutions using coconut dregs residue: Adsorption and characterisation studies. J. Environ. Chem. En. 2: 1912-1919.

Kargi F, Cikla S (2006) Zinc (II) ion recovery by biosorption onto powdered waste sludge (PWS): effects of operating conditions. J. Chem.Technol. Biotechnol. 10: 1661-1668.

Khalaf H, Bouras O, Perrichon V (1997) Synthesis and characterization of Alpillared and cationic surfactant modified Algerian bentonite. Micropor. Mater. 8: 141-150.

Komandel P, Schmidt D, Madejova J, Cicel B (1990) Alteration of smectites by treatments with hydrochloric acid and sodium carbonate solutions. Appl. Clay Sci. 5: 113-122.

Lagergren S (1898) Zur theorie der sogenannten adsorption gelösterstoffe, Kungliga Svenska Vetenskapsakademiens. Handlingar 24: 1-39.

Langmuir I (1918) The adsorption of gases on plane surfaces of glass, mica and platinum. J. Am. Chem. Soc. 40: 1361-1403.

Low KS, Lee CS (2000) Sorption of cadmium and lead from aqueous solutions by spent grain. Proc. Biochem. 36: 59-64.

Mishra PC, Patel RK (2009) Removal of lead and zinc ions from water by low cost adsorbents. J. Hazard. Mater. 168: 319-325.

Nouri J, Mahvi AH, Babaei AA, Jahed GR Ahmad E (2006) Investigation of heavy metals in groundwater. Pak. J. Biol. Sci. 3: 377-384.

Ozcan AS, Ozcan A (2004) Adsorption of aciddyes from aqueous solutions onto acid-activated bentonite. J. Colloid Interface Sci. 276: 39-46.

Rodier J, Legube B, Merlet N, Brunet R (2009) L'analyse de l'eau. Dunod, Paris, France, 1600 p.

Sarı A, Tuzen M, Citak D, Soylak M (2007a) Adsorption characteristics of Cu(II) end Pb(II) onto expanded perlite from aqueous solution. J. Hazard. Mater. 148: 387-395.

Sarı A, Tuzena M, Uluözlüa ÖD, Soylakb M (2007b) Biosorption of Pb(II) and Ni(II) from aqueous solution by Lichen (*Cladoniafurcata*) biomass. Biochem. Eng. J. 37: 151-158.

Schrader ME, Loeb GI (1992) Modern Approaches to Wettability: Theory and Applications. Springer, Boston, USA, 452 p.

Sen TK, Dustin G (2011) Adsorption of Zinc (Zn^{2+}) from aqueous solution on natural bentonite, Desalin. 2-3: 286-294.

Sen TK, Khoo C (2013) Adsorption characteristics of zinc (Zn^{2+}) from aqueous solution by natural bentonite and kaolin clay minerals: A comparative study. CWEEE 2: 1-6.

Sen TK, Sarzali MV (2008) Removal of cadmium metal ion (Cd^{2+}) from its aqueous solution by aluminium oxide: A kinetic and equilibrium study, Chem. Eng. J. 142: 256-262.

Sheta AS, Falatah AM, Al-Sewailem MS, Khaled EM, Salam ASH (2003) Sorption characteristics of zinc and iron by natural zeolite and bentonite. Micropor. Mater. 61: 127-136.

Tomic ZP, Antic-Mladenovic SB, Babic BM (2011) Modification of smectite structure by sulfuric acid and characterization of the modified smectite. J. Agric. Sci. 56: 25-35.

Tunali S, Akar T (2006) Zn (II) biosorption properties of Botrytis cinerea biomass. J. Hazard. Mater. 3: 137-145.

Unlu N, Ersoz M (2006) Adsorption characteristics of heavy metal ions onto a low cost biopolymer sorbent from aqueous solutions. J. Hazard. Mater. 136: 272-280.

Vasconcelos PNM, Lima SW; Silva MLP, Brito ALF, Laborde HM, Rodrigues MGF (2013) Adsorption of zinc from aqueous solutions using modified Brazilian gray clay. Am. J. Anal. Chem. 4: 510-519.

Veli S and Alyüz B (2007) Adsorption of copper and zinc from aqueous solutions by using natural clay. J. Hazard. Mater. 149, 226-233

Yang C, Wang J, Lei M (2010) Biosorption of zinc (II) from aqueous solution by dried activated sludge. J. Environ. Sci. 22: 675-680.

Zwain HM (2012) Comprehensive study on wastewater treatment using low cost adsorbent. LAP Lambert Academic Publishing, Saarbrucken, Germany, 124 p.